Biochimica et Biophysica Acta 1842 (2014) 99–106

Contents lists available at ScienceDirect

Biochimica et Biophysica Acta

journal homepage: www.elsevier.com/locate/bbadis

Increased expression of Myosin binding protein H in the skeletal muscle of amyotrophic lateral sclerosis patients

Antonio Conti [a], Nilo Riva [b,c,f], Mariasabina Pesca [a,i], Sandro Iannaccone [d], Carlo V. Cannistraci [g], Massimo Corbo [h], Stefano C. Previtali [e,c], Angelo Quattrini [f,c], Massimo Alessio [a,*]

[a] Proteome Biochemistry, San Raffaele Scientific Institute, Via Olgettina 58, 20132 Milan, Italy
[b] Department of Neurology, San Raffaele Scientific Institute, Via Olgettina 58, 20132 Milan, Italy
[c] INSPE—Institute of Experimental Neurology, San Raffaele Scientific Institute, Via Olgettina 58, 20132 Milan, Italy
[d] Clinical Neurosciences, San Raffaele Scientific Institute, Via Olgettina 58, 20132 Milan, Italy
[e] Neuromuscular Repair, San Raffaele Scientific Institute, Via Olgettina 58, 20132 Milan, Italy
[f] Experimental Neuropathology, San Raffaele Scientific Institute, Via Olgettina 58, 20132 Milan, Italy
[g] Integrative Systems Biology Lab, Division of Applied Mathematics and Computer Science, King Abdullah University of Science and Technology (KAUST), Thuwal, Saudi Arabia
[h] Department of Neurorehabilitation Sciences, Casa Cura Policlinico, Milan, Italy
[i] Farmaceutical Sciences, Salerno University, Fisciano, SA, Italy

ARTICLE INFO

Article history:
Received 27 June 2013
Received in revised form 18 October 2013
Accepted 24 October 2013
Available online 30 October 2013

Keywords:
Amyotrophic lateral sclerosis
Myosin binding protein H
Skeletal muscle

ABSTRACT

Amyotrophic lateral sclerosis (ALS) is a severe and fatal neurodegenerative disease of still unknown pathogenesis. Recent findings suggest that the skeletal muscle may play an active pathogenetic role. To investigate ALS's pathogenesis and to seek diagnostic markers, we analyzed skeletal muscle biopsies with the differential expression proteomic approach. We studied skeletal muscle biopsies from healthy controls (CN), sporadic ALS (sALS), motor neuropathies (MN) and myopathies (M). Pre-eminently among several differentially expressed proteins, Myosin binding protein H (MyBP-H) expression in ALS samples was anomalously high. MyBP-H is a component of the thick filaments of the skeletal muscle and has strong affinity for myosin, but its function is still unclear. High MyBP-H expression level was associated with abnormal expression of Rho kinase 2 (ROCK2), LIM domain kinase 1 (LIMK1) and cofilin2, that might affect the actin–myosin interaction. We propose that MyBP-H expression level serves, as a putative biomarker in the skeletal muscle, to discriminate ALS from motor neuropathies, and that it signals the onset of dysregulation in actin–myosin interaction; this in turn might contribute to the pathogenesis of ALS.

1. Introduction

Amyotrophic lateral sclerosis (ALS) is characterized by progressive motor neuron degeneration in the brain and spinal cord and by muscle atrophy; collectively, these ailments lead to paralysis and death typically within three to five years of diagnosis [1–4]. Most ALSs are sporadic; only 5–10% of cases are genetically linked, of which 20% show mutation in the Cu/Zn superoxide dismutase SOD1 gene. More recently, other genetic variants, including TARDBP (TAR DNA-binding protein) and FUS (Fused in Sarcoma) mutations, along with C9orf72 (chromosome 9 open reading frame 72) repeat expansions, have been identified in ALS patients. Although several hypotheses have been proposed as to the pathogenesis of ALS, the persistent lack of an effective therapy necessitates a better understanding of the disease mechanisms. Glutamate excitotoxicity, oxidative stress, mitochondrial dysfunction, neurofilament accumulation and other explanations have been linked to ALS, but their precise respective roles in disease pathogenesis still need to be determined [1–4].

Skeletal muscle has commonly been considered the final target of motor neuron degeneration. However, recent findings in genetically linked ALS cases suggest that skeletal muscle is actively involved in the pathogenesis of the disease. A transgenic mouse model expressing mutated $SOD1^{G93A}$ under the transcriptional control of muscle-specific promoter showed progressive muscle atrophy, contractile apparatus alteration and mitochondrial dysfunction without evident signs of motor neuron degeneration [5,6]. The result of this study challenges the idea that motor neuron degeneration, which is caused by transgenic $SOD1^{G93A}$ overexpression in ubiquitous transgenic animals, is the primary cause of muscle atrophy. Muscle atrophy in these animals is one of the earliest detectable events prior to neuromuscular junction alterations, retrogade axonal degeneration, and motor neuron death [3,6–8].

To study specific modifications occurring in proteins of the skeletal muscle at the onset of the disease in ALS patients, we applied a differential

Abbreviations: ALS, amyotrophic lateral sclerosis; CNS, central nervous system; LC-ESI-MS/MS, liquid chromatography electron spray ionization tandem mass spectrometry; 2DE, two-dimensional electrophoresis; WB, Western blot; MyBP-H, Myosin binding protein H; MN, motor neuropathies; M, myopathies

* Corresponding author. Proteome Biochemistry, San Raffaele Scientific Institute, via Olgettina 58, 20132 Milan, Italy. Tel.: +39 02 2643 4725.
E-mail address: m.alessio@hsr.it (M. Alessio).

0925-4439/$ – see front matter © 2013 Elsevier B.V. All rights reserved.
http://dx.doi.org/10.1016/j.bbadis.2013.10.013

proteomic approach to generate a profile of ALS muscle as compared to that of healthy controls, motor neuropathies and myopathies. This approach revealed the increased expression of MyBP-H in ALS samples. The said expression may constitute an early biomarker of ALS disease, and shed light on the disease mechanisms.

2. Materials and methods

2.1. Patients

Following approval of the institutional ethical review board and the granting of informed patient consent, skeletal muscle samples were collected by means of muscle biopsy and stored in the Institute of Experimental Neurology INSPE-Biobank (San Raffaele Scientific Institute, Milan, Italy). Collection was carried out in accordance with the Declaration of Helsinki. Specimens were collected according to the clinical standard procedures, as previously described [9,10], by either gracilis or vastus lateralis muscle biopsy from patients diagnosed with motor neuropathy or ALS or myopathies.

Samples obtained from patients with no pathological alterations and no diagnosis of neuromuscular disorder were used as healthy controls. After biopsy, a cylinder of vastus lateralis or gracilis muscle tissue (10 mm long and 4 mm wide) was rapidly frozen by immersion in isopentane and kept cool in liquid nitrogen.

The groups analyzed were: sporadic amyotrophic lateral sclerosis (sALS, n = 17), motor neuropathies (MN, n = 9), myopathies (M, n = 6) and healthy controls (CN, n = 11); Table 1 describes features in detail. All ALS and MN patients were at their first diagnosis and were drug-free. Neurological diagnosis was performed in accordance with standard clinical neurophysiological and neuropathological criteria, as described in [9,11]. Exclusion criteria included: HIV or Hepatitis C virus positive; previous cerebral ischemic events; deep metabolic deficit and other neurodegenerative diseases.

2.2. Sample preparation, two-dimensional electrophoresis (2DE), image analysis, mass spectrometry (MS), SDS-PAGE and Western blot

Analysis used skeletal muscle homogenate. Muscle biopsy (100 mg each sample) was minced, resuspended in a 2 ml rehydration solution (urea 8 M, chaps 4% w/v) and then homogenized with Dounce equipment. After centrifugation, the supernatant was collected and intact pieces of tissue were thus discarded. Protein concentration was determined by the Bradford (BioRad) method, and aliquots were stored at −80 °C. Each homogenate sample (100 μg) was resuspended in a buffer containing urea (8 M), CHAPS (4% w/v), DTT (65 mM), 0.2% v/v IPG-buffer 3–10 NL (GE Healthcare, Milan, Italy) and 0.05% Bromophenol blue, and used for the generation of 2DE maps as described in [12,13]. Isoelectric focusing was performed by using either 7 or 18 cm pH 3–10 non-linear gel strips (GE-Healthcare), while second dimension was performed on 9–16% gradient SDS-PAGE. Gels were stained with MS-compatible silver staining, and images were acquired at high resolution with the ProXPRESS system (Perkin Elmer). The protein resolved on 7 cm small 2DE gels were electro-transferred to nitrocellulose membrane for Western blot (WB) analysis (see below). Images of 2DE profiles underwent software-assisted analysis by means of Progenesis SameSpot (Nonlinear Dynamics), and the identified differentially expressed protein spots (ANOVA $p < 0.05$, as analyzed by Progenesis Stat) were excised from gels, reduced, alkylated, and in-gel digested overnight with bovine trypsin (Roche Diagnostics Corp.), as previously described [14]. Five microliters of digested sample, acidified to 1% with Formic Acid, were injected into a capillary chromatographic system (Agilent1100 Series) that was equipped with a Nano Pump (Agilent). Peptide separation occurred on a homemade RP C18 nano column. The eluting peptides were ionized by a nanoESI on-line source and analyzed on an API QStar PULSAR (AB-Sciex, Toronto, Canada) mass spectrometer. Full scan mass spectra ranging from m/z 350 to 1600 were collected and, for each MS spectrum, the two most intense doubly and triply charged ion peaks were selected for fragmentation. MS/MS spectra data files from each chromatographic run were combined and converted to Mascot generic files with Mascot.dll (version 2.2.07) by means of Analyst QS 1.1 (AB Sciex). All MS/MS samples were analyzed with a MASCOT engine that searched the UniProt_CP_human_2012_11 database. We used a peptide mass tolerance of 200 ppm and 0.3 Da respectively for precursor and fragment ions. The other search parameters were: two missed cleavages allowed; oxidation of Methionine as a variable modification, and carbamidomethylation as a fixed modification.

The validation of differential protein expression levels was undertaken by WB analysis performed on 10 μg muscle homogenate biopsy sample lysates, and used antibodies specific for the identified proteins, as described in [12,13]. The antibodies used were: anti-MyBP-H,

Table 1
Patient and control features.

CN				sALS				MN					M				
	Sex	Age	Mus		Sex	Age	Mus		Sex	Age	Mus	Diagn		Sex	Age	Mus	Diagn
CN 1	F	45	v	ALS 1	F	50	g	MN 1	M	39	g	MMNCB [c]	M 1	F	37	v	DM [a/c]
CN 2	F	32	v	ALS 2	M	46	g	MN 2	M	57	g	MMNCB [c]	M 2	F	58	v	NM [a/c]
CN 3	F	36	v	ALS 3	M	42	g	MN 3	M	57	g	MMNCB [c]	M 3	F	31	v	T [a]
CN 4	M	24	v	ALS 4	F	50	g	MN 4	M	65	g	MMN [c]	M 4	F	31	v	T [a]
CN 5	F	35	v	ALS 5	M	54	g	MN 5	M	60	g	MN [c]	M 5	F	52	v	MD [c]
CN 6	M	55	v	ALS 6	M	63	g	MN 6	M	60	g	MN [sa]	M 6	M	27	v	MD [c]
CN 7	M	35	v	ALS 7	F	48	g	MN 7	M	76	g	MN [c]					
CN 8	F	48	v	ALS 8	F	65	g	MN 8	F	45	g	MN [a]					
CN 9	F	43	v	ALS 9	M	51	g	MN 9	F	47	g	MN [c]					
CN 10	F	45	v	ALS 10	M	54	g										
CN 11	M	60	g	ALS 11	M	55	g										
				ALS 12	F	65	g										
				ALS 13	M	70	g										
				ALS 14	M	55	g										
				ALS 15	F	56	v										
				ALS 16	F	68	v										
				ALS 17	M	74	v										
	4M/7F				10M/7F				7M/2F					1M/5F			
m ± sd		41.6 ± 10.5				56.8 ± 9.1						56.2 ± 11.2					39.3 ± 12.7

Gender: no statistical differences among groups (Fischer's exact test) except for MN vs. M ($p = 0.0406$).
Age: statistical differences (Student's t-test) have been found for CN vs. ALS ($p = 0.0004$), CN vs. MN ($p = 0.0077$), ALS vs. M ($p = 0.0015$), and MN vs. M ($p = 0.0177$).
CN = healthy subjects; sALS = sporadic amyotrophic lateral sclerosis; MN = motor neuropathies; M = myopathies. Mus = muscle; v = vastus muscle; g = gracilis muscle; Diagn = diagnosis; m = mean; sd = standard deviation. MMNCB = multifocal motor neuropathy with conduction blocks; MMN = multifocal motor neuropathy. DM = dermatomyositis; NM = necrotizing myositis; T = toxic; MD = muscular dystrophy. [c] = chronic; [sa] = subacute; [a] = acute.

-tropomyosin, -troponin, -α-actin, -myosin heavy chain, -neonatal myosin, -neuropolypeptide H3 (all from Abcam), and -myosin light chain (Cell Signaling). WB analysis was also performed to investigate the expression of proteins hypothetically related to MyBP-H's function. The antibodies used were: anti-myosin binding protein-C (MyBP-C), -thyroid transcription factor 1 (TTF1), -cofilin2 (from Abcam), -LIM domain kinase 1 (LIMK1), and -Rho kinase 2 (ROCK2) (from Cell Signaling). Secondary HRP-conjugated antibodies were from Dako. Antibody reactivity was quantified by densitometric analysis (Molecular Dynamics Personal SI Laser Densitometer) and normalized by total protein loading and actin expression, as in [15].

2.3. Immunoprecipitation

Homogenate lysate proteins (100 μg) were subjected to immunoprecipitation with 1 μg of either monoclonal antibody anti-MyBP-H (Abcam 55561) or the rabbit polyclonal serum anti-MyBP-H (Abcam 98187) coupled to protein G-Sepharose (GE-Healthcare). Immunoprecipitates were washed and bound proteins were eluted by incubation of the beads for 4 min at 99 °C together with Laemmli buffer. Proteins were then resolved by SDS-PAGE and analyzed by WB with both monoclonal anti-MyBP-H and anti-ROCK2 antibodies.

2.4. Lambda phosphatase treatment

Lambda Protein Phosphatase (λ-PPase) (New England BioLabs) treatment was performed as described in [16] with modifications. In brief, muscle homogenates were resuspended in lysis buffer (1% w/v NP-40, 1% w/v SDS, 50 mM Tris pH 7.6, 150 mM NaCl, protease inhibitor cocktail); lysate (60 μg of protein) was brought to a final volume of 100 μl with distilled water and supplemented with 10 μl of 20 mM $MnCl_2$ solution and 10 μl of λ-PPase reaction buffer (New England BioLabs). Each mixture was supplemented with λ-PPase (1000 units), and incubated for 12 h at 30 °C. Proteins were acetone precipitated (80% acetone final concentration) at −20 °C for 12 h and used for SDS-PAGE and WB analysis.

2.5. Immunofluorescence

Skeletal muscle biopsies were frozen in cold 2-methylbutane and then in liquid nitrogen and stored at −80 °C. Ten micrometer sections were cut by means of a Leica cryostat and then mounted on glass microscope slides. Sections were either used immediately or stored at −80 °C prior to usage. Tissue sections were blocked for 2 h at 20 °C in PBS with 0.3% BSA, 0.3% Triton and 5% goat serum; they were then incubated with the primary antibody for 2 h at 20 °C or 12 h at 4 °C. Antibodies used were: anti-MyBP-H, anti-fast myosin skeletal heavy chain and anti-slow myosin skeletal heavy chain (Abcam). After washing with four changes of blocking buffer without serum for a total of 1 h, the sections were incubated with fluorochrome-conjugated secondary antibody for 1 h at 20 °C (Invitrogen). The sections were finally washed for a total of 1 h, mounted with Mowiol (Hoechst), and analyzed with OLYMPUS BX51 fluorescence microscope and a Leica DC 480 camera.

2.6. Statistical analysis

Gender distribution was analyzed by Fisher's exact test and two-tailed p value. Continuous data were evaluated by unpaired Student's t-test, if the data passed the normality test for Gaussian distribution as assessed by the Kolmogorov–Smirnov test; alternatively, they were evaluated by Mann–Whitney test. Two-tailed p value was used for the comparison of two means and standard error. Covariance was analyzed by Kruskal–Wallis test with Dunn's Multiple Comparison post-test analyses. In all analyses, $p < 0.05$ was considered to be statistically significant. The analysis was performed with Prism V4.03 software (GraphPad Inc.).

3. Results

3.1. Protein differential expression in the muscle of ALS patients

Muscle biopsy protein extracts from CN ($n = 10$), ALS ($n = 14$) and MN ($n = 9$) subjects were used to generate 2DE maps. Image analysis showed 20 spots differentially expressed with statistical significance (ANOVA <0.05); for eleven of these spots, protein identification was assigned by MS analysis, which identified ten different proteins (Fig. 1) (Supplemental materials SM—Table 1). The expression level of five proteins (α-actin, actin prepeptide, myosin light chain 2, tropomyosin 3 isoform 1, β-tropomyosin) was lower in ALS than in CN, whereas the expression of one protein, MyBP-H, was higher in ALS than in CN. Comparative analysis of ALS and MN revealed that the expression of 3 proteins (MyBP-H, creatine kinase muscle, glyceraldehyde-3-phosphate dehydrogenase) was higher in ALS than in CN, and that the expression of 2 proteins (neuropolypeptide H3, β-myosin heavy chain) was lower in ALS than in CN (SM—Table 1).

Validation of the observed protein expression changes performed by WB analysis with specific antibodies failed to confirm statistical significance for 9 out of 10 proteins (not shown). This was probably due to the fact that most of the differentially expressed spots proved to be protein fragments. In contrast, WB validation experiments confirmed significant expression changes for MyBP-H [17]; we accordingly focused our attention on this protein.

3.2. Increased expression of Myosin binding protein H in ALS patients

Western blot analysis showed that the expression level of MyBP-H was able to discriminate between varying populations as inferred by Kruskal–Wallis test ($p < 0.0001$). MyBP-H expression was higher in ALS than in CN and/or MN patients, and the differences, as evaluated with Dunn's Multiple Comparison post-test analysis (respectively $p < 0.001$ and $p < 0.01$) (Fig. 2A and B), proved to be significant. MyBP-H expression in CN and MN was generally weak, and for some samples, undetectable (Fig. 2A). MyBP-H expression was not related to the origin of muscle specimen, namely, vastus versus gracilis, since the molecule was highly expressed in ALS patients and weakly or not-expressed in CN and MN, regardless of the type of muscles. However, three MN patients (MN6, MN8 and MN9) showed MyBP-H expression levels that were comparable to those of ALS patients with lower MyBP-H expression (Fig. 2B). We accordingly investigated a further control group of patients in whom muscular damage was not related to neuronal diseases (chronic and acute myopathies). MyBP-H expression proved to be higher in the myopathy (M) cohort than in controls, albeit to a lesser extent than in ALS patients (Fig. 2A and B). These results likewise indicate that MyBP-H expression was not related to a specific muscle source, as both CN and M specimens derived mainly from the vastus muscle. However, the size of the myopathy cohort was insufficient for the MyBP-H increase in question to be granted statistical significance. Given the higher degree of muscular damage in myopathic as compared to ALS samples, the relatively lower increase in MyBP-H suggests that its expression does not merely correlate with muscular damage. That the expression of MyBP-H in the skeletal muscle of ALS patients differed from that in control groups was confirmed by immunofluorescence on muscle cryo-sections from the same specimens as those used for 2DE analysis. In agreement with the results obtained by WB analysis, staining for MyBP-H was positive in ALS and in myopathy samples, but was negative or very weakly positive in CN and MN samples (Fig. 2C).

We then applied 2DE and WB to investigate whether MyBP-H in ALS patients had undergone biochemical changes as a result of post-translational modifications. Results showed no variations between the electrophoretic mobility patterns respectively found in ALS, CN and MN subjects (SM—Fig. 1).

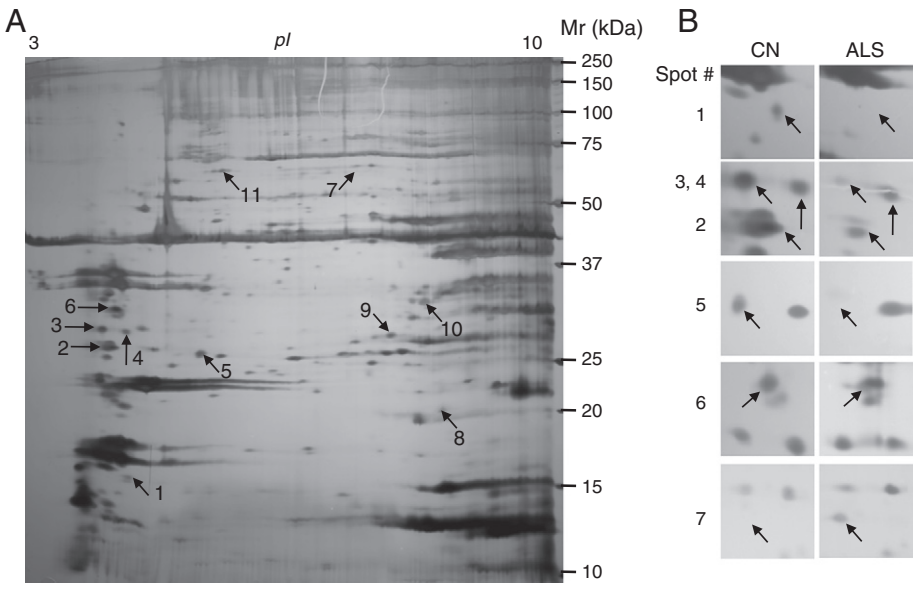

Fig. 1. Protein differential expression in ALS patients muscle. A) Two-dimensional electrophoresis map of muscle homogenate from a representative ALS patient. Proteins were separated by *pI* in the first dimension on a pH 3–10 NL, and by molecular weight in the second dimension on a 9–16% acrylamide gradient SDS-PAGE. Protein spots were revealed by silver staining. The protein spots that follow image analysis showed differential expression among patients and controls are indicated by arrows. Spot numbers are referred to mass spectrometry protein identification reported in Supplemental materials Table 1. B) Comparisons of protein spots expression in control healthy subjects (CN) and ALS patients. Enlargements of the 2DE areas of some representative spots.

The literature has described two related members of the family of myosin binding proteins, namely MyBP-C and MyBP-H [18,19]. These proteins, which differ in terms of the N-terminal domains, are both associated, via the C-terminal domain, with myosin in the A-band of the thick filaments in myofibrils [18]. We accordingly investigated whether MyBP-C expression too was affected in ALS muscles. WB analysis revealed no changes in expression (SM—Fig. 2).

3.3. Increased expression of MyBP-H in ALS is not associated with fast twitch muscle fiber enrichment

In chicken and rabbit skeletal muscles, MyBP-H has been reported to be primarily associated with fast twitch muscle fibers [20,21]. As we analyzed all the muscle samples collected at disease onset, we investigated whether the anomalous expression of MyBP-H in damaged ALS muscles

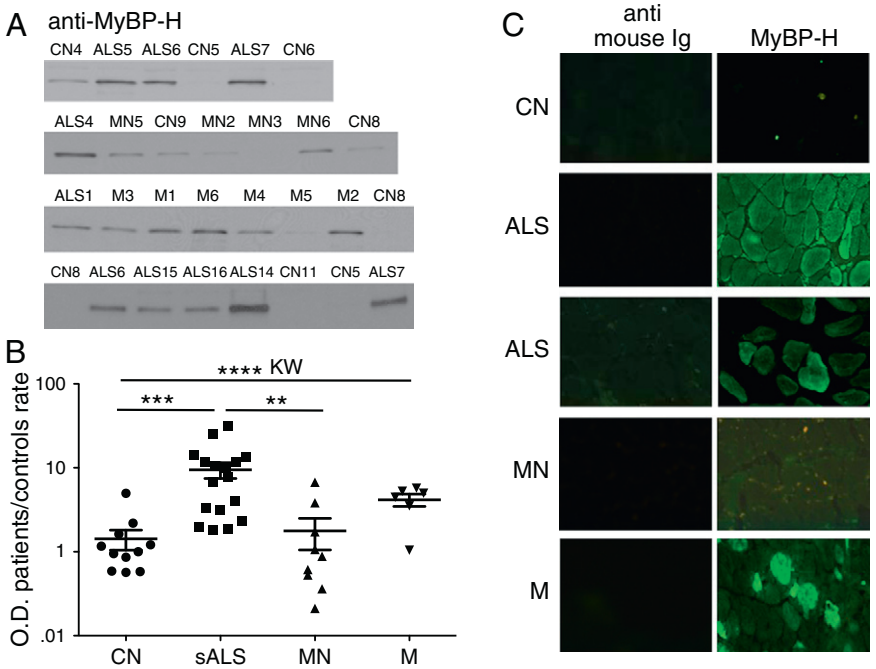

Fig. 2. Myosin binding protein H increased expression in ALS patients. A) Western Blot analysis performed with anti-MyBP-H antibody on skeletal muscle homogenate from sporadic ALS patients (sALS, n = 17), healthy subjects (CN, n = 11), motor neuropathies patients (MN, n = 9) and myopathies patients (M, n = 6). B) Analysis of WB signal optical density (O.D.) reported as patient vs. control rate. Data were analyzed by covariance analysis performed with the Kruskal–Wallis test (****KW, $p < 0.0001$) and post-analysis test between individual groups with the Dunn's Multiple Comparison Test (**, $p < 0.01$; ***, $p < 0.001$). C) Immunofluorescence staining of MyBP-H on transverse sections of skeletal muscle biopsies of representative highly expressing MyBP-H ALS patients (ALS5 and 6, upper and lower, respectively), healthy subject (CN5), motor neuropathy (MN3) and myopathy (M2).

reflected an aberrant manifestation of fast twitch muscle fibers [22]; these latter co-occurred with an unsuccessful attempt at muscular regeneration. The transition of muscle fiber phenotype from slow to fast can indeed be induced by denervation/re-innervation neuromuscular activity [23]. Immunofluorescence against slow- and fast-myosin fibers performed on ALS patients, healthy subjects (CN) and MN patients showed comparable percentages of fast-myosin fibers in the three groups, which suggests that MyBP-H expression was not associated with fast twitch muscle fiber enrichment in ALS patients (Fig. 3A and B). Muscular regeneration is associated with the transitional expression of neonatal myosin before the switch to adult isoforms that takes place under the control of reconstituted nerve activity [22]. Western blot analysis showed no significant differences in the respective expression levels of neonatal myosin in ALS, CN and MN (SM—Fig. 3).

3.4. ROCK2, LIMK1 and cofilin2 levels increase in ALS samples

In lung adenocarcinoma cell lines, MyBP-H has been reported to be a transcriptional target of TTF-1 and to physically interact with Rho kinase 1 (ROCK1); this interaction inhibits MyBP-H activity, which in turn affects actin–myosin interaction and cell motility [24]. We accordingly investigated whether MyBP-H expression in ALS skeletal muscle is associated with increased expression of TTF-1, and whether MyBP-H functionally interacted with ROCK kinases. Western blot analysis showed the level of TTF-1 expression in ALS muscles to be low and comparable to that observed in CN (data not shown). Interestingly, ROCK2, the ROCK isoform expressed in muscle [25,26], was significantly higher in ALS than in CN samples ($p = 0.0298$ by Mann–Whitney test) (Fig. 4A).

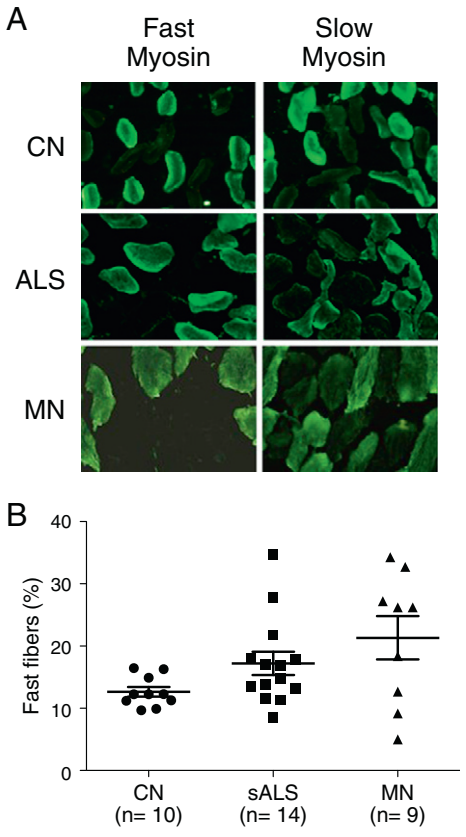

Fig. 3. Presence of slow- and fast-myosin fibers. A) Immunofluorescence staining of slow- and fast-myosin fibers performed on transverse sections of skeletal muscle biopsies of representative CN, sALS and MN. B) Analysis of the percentage of fast-myosin fibers present in three different fields of immunostaining performed on transverse sections of healthy subjects (CN, $n = 10$), sporadic ALS patients (ALS, $n = 14$), and motor neuropathies patients (MN, $n = 9$). No statistical differences occurred as inferred by covariance analysis performed with the Kruskal–Wallis test and Dunn's post-analysis test.

We therefore investigated whether ROCK2 interacted with MyBP-H in ALS samples. Co-immunoprecipitation experiments performed respectively with monoclonal and polyclonal anti-MyBP-H antibodies followed by WB with anti-ROCK2 revealed no physical interaction between the two molecules (SM—Fig. 4).

Given the functional role that ROCK2 plays in actin–myosin interaction and function, the increased expression in ALS prompted us to investigate the downstream targets of its kinase activity. The ROCK pathway leads to actin–myosin filament assembly, in which contractile force is generated by the phosphorylation of numerous substrate proteins [27]. ROCKs exert their kinase activity through two differing target pathways: 1) phosphorylation of LIM kinases, whose specific activity on cofilin increases and causes inactivation of cofilin's actin depolymerization function; this in turn results in actin filament stabilization; 2) phosphorylation of the regulatory myosin light chain (M-RLC), and phosphorylation of the myosin-binding subunit 1 (MYPT1), which inhibits myosin phosphatases; this in turn results in myosin binding to the actin filament and hence to the initiation of contraction [27].

Interestingly, WB analysis revealed higher expression of both LIMK1 and cofilin2 in ALS than in CN muscle samples ($p = 0.0004$ by Mann–Whitney test and $p = 0.0065$ by Student's t test, respectively) (Fig. 4B and C). In contrast, no changes in the expression levels were detected in ALS samples for proteins belonging to the M-RLC downstream pathway (data not shown).

3.5. A non-phosphorylated LIMK1 isoform accumulates in ALS muscles

As evidenced in Fig. 4B, LIMK1 in ALS patients showed two bands of similar intensity, while in CN the upper band markedly prevailed over the non-detectable or very faint lower band. Optical density analysis showed that the expression level of the upper band was similar in both CN and ALS samples ($p = 0.1388$ by Mann–Whitney), whereas the lower band was responsible for the relative increase observed in ALS samples ($p = 0.0018$ by Mann–Whitney test) (Fig. 5A). Treatment with lambda phosphatase (λ-PPase) induced the appearance of a lower band in CN and an accumulation of the signal in the lower band in ALS patients. This finding indicates that the upper band is the phosphorylated isoform of LIMK1, which prevails in healthy subjects, and that a non-phosphorylated isoform of LIMK1 had accumulated in ALS patients (Fig. 5B). Use of WB with specific antibodies did not enable us to detect cofilin2 phosphorylation in the samples (data not shown); however, 2DE and WB analysis indirectly suggested that, downstream to LIMK1, cofilin2 was less phosphorylated in ALS patients than in CN subjects. This feature was evidenced by the fact that spot acidity was lower in ALS than in CN samples (Fig. 6). In contrast, the same analysis suggested that phosphorylation of the ROCK downstream-target MLC2 protein in ALS samples does not differ from that in ALS compared to CN samples, since the MLC2 isoelectric points were identical in the two groups (SM—Fig. 5).

These results show that the increased expression of MyBP-H in ALS samples is associated with abnormal expression of ROCK2 and the downstream targets LIMK1 and cofilin2.

4. Discussion

To date, muscle has played a limited role in the identification of biomarkers in ALS, even though the demonstration of muscular abnormalities made such a role conceivable [28,29]. Of particular pertinence in this respect are the reports showing that motor neuron degeneration might occur in a retrograde fashion as a consequence of the early destabilization of the neuro-muscular junction (NMJ) ([29] and references therein) [5,6].

The main finding of this work is that, at disease onset, the skeletal muscles of ALS patients show increased expression of a putative marker, namely MyBP-H, that is already able at onset to distinguish ALS patients

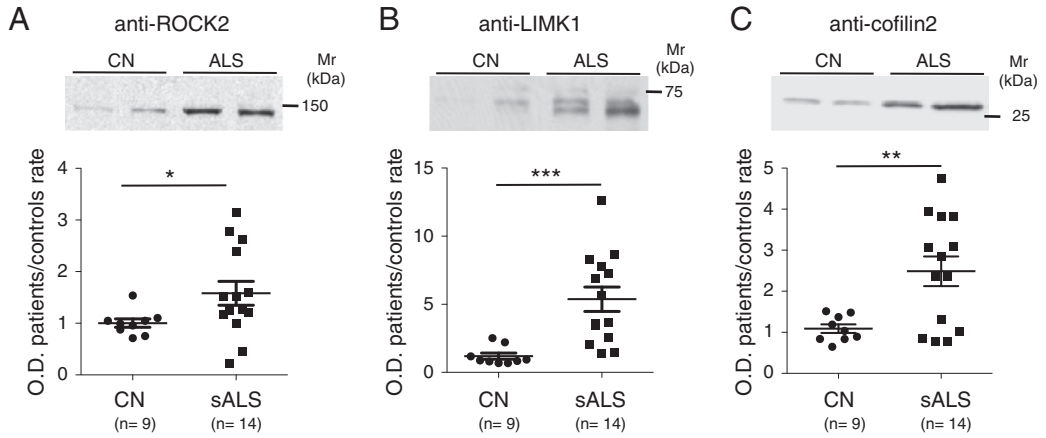

Fig. 4. Western blot analysis of ROCK2, LIMK1 and cofilin2 expression. Analysis was performed on skeletal muscle homogenate from sporadic ALS patients (ALS) and healthy subjects (CN). Analysis of WB signal optical density (O.D.) obtained with antibodies specific for ROCK2 (A), LIMK1 (B) and cofilin2 (C) is reported as patient vs. control rate. Data were analyzed by Mann–Whitney test (A, $p = 0.0298$; B, $p = 0.0004$) and by Student's t test (C, $p = 0.0065$).

both from healthy subjects and, more importantly, from the patients of other similarly incipient motor neuropathies.

MyBP-H is a myofibrillar protein constituent of vertebrate skeletal muscle of about 55 kDa. Located in the A-band of the myofibrils, it is closely associated with the thick filaments, but its primary association is with the fibers of fast twitch muscles [18–21]. A functional role for MyBP-H has not yet been described. A further associate of the thick filament of myosin is MyBP-C, another member of the family of myosin binding proteins [18,19]; this member of the family shares MyBP-H's significant homology at the carboxyl-terminal domains, the region involved in myosin binding. Unlike MyBP-C, MyBP-H lacks the amino-terminal region, which is responsible for the regulation of myosin contractile functions [18,19,30]. The demonstration that the myosin binding domain of MyBP-C can replace that of MyBP-H without affecting its localization makes it conceivable that MyBP-H partially compensates for the lack of MyBP-C [18]. However, the observation that MyBP-C expression was similar in ALS, MN and CN groups rules out this hypothesis. The possibility that MyBP-H expression was related to the degree of muscular damage was also excluded on the grounds that the myopathic samples, in which muscular damage was higher than in ALS samples, showed an increase in MyBP-H compared to CN that was lower than that found in ALS patients. This observation suggests that the over-expression of MyBP-H might not depend, or might only partially depend, on muscular damage.

The reported association of MyBP-H with fast twitch fibers in skeletal muscle of chicken and rabbit [20,21] led us to hypothesize that its over-expression in sALS could be related to an attempt at regeneration that the muscle made in the early phase of the disease (i.e., when NMJ alteration occurred). The presence of fast twitch muscle fibers and neonatal myosin have been associated with denervated-regenerating muscle [22], and single muscle fiber contractile analysis has demonstrated that fast-twitch muscle fibers and neuromuscular junctions are preferentially affected by ALS-induced denervation [31]. Although the expression in ALS muscles both of fast myosin and of neonatal myosin did

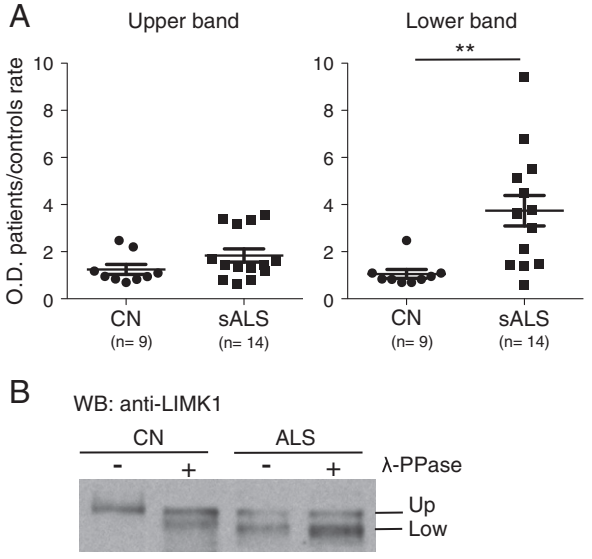

Fig. 5. Non-phosphorylated isoform of LIMK1 is accumulated in ALS patients. A) Analysis of WB signal optical density (O.D.) of upper and lower bands revealed with anti-LIMK1 in healthy subjects (CN) and sporadic ALS (sALS) (see Fig. 4B). Data, reported as patient vs. control rate, were analyzed by Mann–Whitney test (**$p = 0.0018$). B) WB analysis of LIMK1 dephosphorylation in CN and sALS muscle homogenate following λ-phosphatase (λ-PPase) treatment. Lower band signal appearance in CN and accumulation of the signal in the lower band in ALS as consequence of λ-PPase treatment indicated that the upper band is the phosphorylated isoform of LIMK1 that is prevalent in CN.

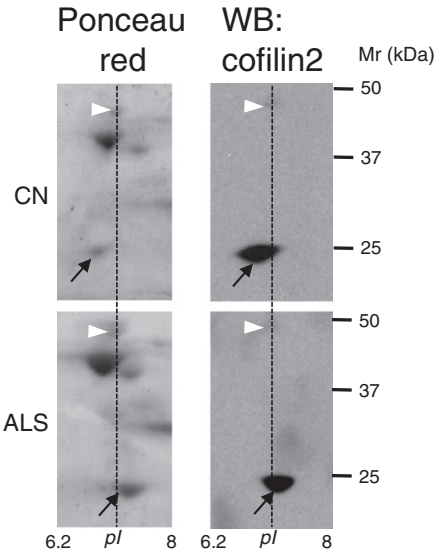

Fig. 6. A Less acidic isoform of cofilin2 is expressed in ALS patients. 2DE analysis and WB performed with anti-cofilin2 on muscle homogenate of a representative healthy subject (CN) and sporadic ALS patients respectively. Electrophoretic mobility feature of cofilin2 spots, indicated by the black arrows on the Ponceau red stained membranes, and the signals revealed by the anti-cofilin2 (black arrows on WB) showed a less acidic cofilin2 in ALS patients compared to healthy subjects, which in turn may suggest a reduced/absent phosphorylation in ALS patients. The white head-arrows indicated the non-specific signal visible in the WB that has been used for image alignment.

not differ from analogous expression in MN and CN muscles, our observations suggest that changes in MyBP-H expression precede changes in the myosin chain composition consequences of denervation.

The observations we made in ALS patients are supported both at mRNA and protein levels in ALS animal models. An increase in MyBP-H expression at the transcriptional level has been reported in the muscle of SOD1^{G86R} transgenic mice ALS model [32]. The increase was observed in the early stage of disease onset, when the first signs of peripheral denervation and muscular atrophy are not caused by degeneration of the motor neuron, but are rather the result of axonal dysfunction [32]. A similar conclusion was inferred by the observation of the induction of MyBP-H mRNA expression in mice 7 days after sciatic nerve axotomy, prior to motor neuron death [32]. In these animal models, the induction of genes implicated in myogenesis and cytoskeleton organization has been proposed as playing an important role in stimulating the regenerative capacity of muscle during the first steps of atrophy [32]. At a protein level, an increase in MyBP-H expression has been reported in the muscle of 7-week-old SOD1^{G93A} transgenic mice models for ALS, when overt clinical symptoms at hindlimbs, like weakness and tremor, have yet to occur [33]. Interestingly, decreased MyBP-H expression in 14-week-old SOD1^{G93A} mice occurred exclusively in the gastrocnemius muscle of pathologically compromised hindlimbs, but not in the triceps muscle of the then not compromised forelimbs [33]. Furthermore, increased mRNA expression of MyBP-H was reported in all muscles of rats pharmacologically paralyzed by post-synaptic block of neuromuscular transmission (NMB) [34]. In response to NMB, MyBP-H showed a transcriptional regulation that differed completely from that of all other myofibrillar proteins, which are down-regulated. This finding suggests that MyBP-H up-regulation might represent an early sign of muscle regeneration [34]. Interestingly, the ALS samples submitted to proteomics analysis revealed a similar behavior: while several myofibrillar proteins were down-regulated, MyBP-H expression exclusively increased. It is noteworthy that, during the muscular wasting/atrophy that occurs in the absence of NMJ alteration, as in response to food deprivation, MyBP-H expression was reported as having decreased [35,36]. The results of our study are consistent with a model whereby muscular alteration is an early pathological event in ALS [5,6,8]; whether this event is associated with NMJ alteration and is independent from motor neuron degeneration remains to be defined.

From the molecular point of view, MyBP-H negatively regulates actomyosin organization in non-muscle cells, and thus inhibits both the phosphorylation of myosin regulatory light chain (M-RLC) and the assembly of non-muscle myosin heavy chain IIA (NMHC IIA) [24,37]. The inhibitory function is exerted by an interaction with both NMHC IIA and ROCK1, the latter being the kinase responsible for M-RLC phosphorylation [24,37]. ROCK1 and ROCK2 are key regulators of cellular actomyosin contractility by means of the phosphorylation of substrates, which included LIMK kinases and M-RLC2 [38,39]. In non-muscle cell, the ROCK1 negative regulatory function exerted by MyBP-H resulted in a lack of LIMK phosphorylation/activation, which in turn promoted the activation of the actin-depolymerizing factor cofilin [24]. Our findings show that increased expression of MyBP-H co-occurs with altered expression of ROCK2, as well as with altered expression/phosphorylation of LIMK1 and cofilin2; these findings might suggest that, analogously with non-muscle cells, skeletal muscle might be characterized by a functional relation between these actomyosin regulators. However, without evidence of reduced ROCK2 kinase activity, it cannot be excluded that the observed alteration in LIMK1 phosphorylation derives from a different signaling pathway, since LIMK1 is the target of several kinases. Furthermore, the lack of molecular interaction between MyBP-H and ROCK2 prevents us from concluding whether increased expression of MyBP-H affects ROCK2 kinase activity and whether it is directly responsible for the molecular changes observed. Indeed, we cannot exclude that MyBP-H over-expression exerts its function through a completely different mechanism whereby myosin binding properties of MyBP-H attempt to stabilize myosin filaments.

5. Conclusions

The increased expression of MyBP-H in the skeletal muscle of ALS patients might possibly be a marker for the purposes of differential diagnosis, in that the increase may reflect muscular alteration and, possibly, an attempt at regeneration. To understand why the compensatory mechanism fails will be the next step in research. The generation of a transgenic animal model would help research to establish whether MyBP-H plays a directly detrimental or proactive role in these mechanisms.

Acknowledgements

This work was supported by MoH, RF07-ALS. The authors declare no conflict of interest.

Appendix A. Supplementary data

Supplementary data to this article can be found online at http://dx.doi.org/10.1016/j.bbadis.2013.10.013.

References

[1] L.P. Rowland, N.A. Shneider, Amyotrophic lateral sclerosis, N. Engl. J. Med. 344 (2001) 1688–1700.
[2] J.D. Mitchell, G.D. Borasio, Amyotrophic lateral sclerosis, Lancet 369 (2007) 2031–2041.
[3] A. Musaro, State of the art and the dark side of amyotrophic lateral sclerosis, World J. Biol. Chem. 1 (2010) 62–68.
[4] A.J. Pratt, E.D. Getzoff, J.J. Perry, Amyotrophic lateral sclerosis: update and new developments, Degener. Neurol. Neuromuscul. Dis. 2012 (2012) 1–14.
[5] G. Dobrowolny, M. Aucello, E. Rizzuto, S. Beccafico, C. Mammucari, S. Boncompagni, S. Belia, F. Wannenes, C. Nicoletti, Z. Del Prete, N. Rosenthal, M. Molinaro, F. Protasi, G. Fano, M. Sandri, A. Musaro, Skeletal muscle is a primary target of SOD1^{G93A}-mediated toxicity, Cell Metab. 8 (2008) 425–436.
[6] M. Wong, L.J. Martin, Skeletal muscle-restricted expression of human SOD1 causes motor neuron degeneration in transgenic mice, Hum. Mol. Genet. 19 (2010) 2284–2302.
[7] M.E. Gurney, H. Pu, A.Y. Chiu, M.C. Dal Canto, C.Y. Polchow, D.D. Alexander, J. Caliendo, A. Hentati, Y.W. Kwon, H.X. Deng, et al., Motor neuron degeneration in mice that express a human Cu,Zn superoxide dismutase mutation, Science 264 (1994) 1772–1775.
[8] G. Dobrowolny, M. Aucello, A. Musaro, Muscle atrophy induced by SOD1^{G93A} expression does not involve the activation of caspase in the absence of denervation, Skelet. Muscle 1 (2011) 3.
[9] N. Riva, S. Iannaccone, M. Corbo, C. Casellato, B. Sferrazza, A. Lazzerini, M. Scarlato, F. Cerri, S.C. Previtali, E. Nobile-Orazio, G. Comi, A. Quattrini, Motor nerve biopsy: clinical usefulness and histopathological criteria, Ann. Neurol. 69 (2011) 197–201.
[10] S. Benedetti, E. Bertini, S. Iannaccone, C. Angelini, M. Trisciani, D. Toniolo, B. Sferrazza, P. Carrera, G. Comi, M. Ferrari, A. Quattrini, S.C. Previtali, Dominant LMNA mutations can cause combined muscular dystrophy and peripheral neuropathy, J. Neurol. Neurosurg. Psychiatry 76 (2005) 1019–1021.
[11] B.R. Brooks, R.G. Miller, M. Swash, T.L. Munsat, El Escorial revisited: revised criteria for the diagnosis of amyotrophic lateral sclerosis, Amyotroph. Lateral Scler. Other Motor Neuron Disord. 1 (2000) 293–299.
[12] A. Conti, P. Ricchiuto, S. Iannaccone, B. Sferrazza, A. Cattaneo, A. Bachi, A. Reggiani, M. Beltramo, M. Alessio, Pigment epithelium-derived factor is differentially expressed in peripheral neuropathies, Proteomics 5 (2005) 4558–4567.
[13] A. Conti, S. Iannaccone, B. Sferrazza, L. De Monte, S. Cappa, D. Franciotta, S. Olivieri, M. Alessio, Differential expression of ceruloplasmin isoforms in the cerebrospinal fluid of amyotrophic lateral sclerosis patients, Proteomics Clin. Appl. 2 (2008) 1628–1637.
[14] V. Corti, A. Cattaneo, A. Bachi, R.E. Rossi, G. Monasterolo, C. Paolucci, S.E. Burastero, M. Alessio, Identification of grass pollen allergens by two-dimensional gel electrophoresis and serological screening, Proteomics 5 (2005) 729–736.
[15] I. Romero-Calvo, B. Ocon, P. Martinez-Moya, M.D. Suarez, A. Zarzuelo, O. Martinez-Augustin, F.S. de Medina, Reversible Ponceau staining as a loading control alternative to actin in Western blots, Anal. Biochem. 401 (2010) 318–320.
[16] F. Di Modugno, L. DeMonte, M. Balsamo, G. Bronzi, M.R. Nicotra, M. Alessio, E. Jager, J.S. Condeelis, A. Santoni, P.G. Natali, P. Nistico, Molecular cloning of hMena (ENAH) and its splice variant hMena+11a: epidermal growth factor increases their expression and stimulates hMena+11a phosphorylation in breast cancer cell lines, Cancer Res. 67 (2007) 2657–2665.
[17] K.T. Vaughan, F.E. Weber, T. Ried, D.C. Ward, F.C. Reinach, D.A. Fischman, Human myosin-binding protein H (MyBP-H): complete primary sequence, genomic organization, and chromosomal localization, Genomics 16 (1993) 34–40.
[18] R. Gilbert, J.A. Cohen, S. Pardo, A. Basu, D.A. Fischman, Identification of the A-band localization domain of myosin binding proteins C and H (MyBP-C, MyBP-H) in skeletal muscle, J. Cell Sci. 112 (Pt 1) (1999) 69–79.

[19] C.C. Witt, B. Gerull, M.J. Davies, T. Centner, W.A. Linke, L. Thierfelder, Hypercontractile properties of cardiac muscle fibers in a knock-in mouse model of cardiac myosin-binding protein-C, J. Biol. Chem. 276 (2001) 5353–5359.
[20] M. Bahler, H.M. Eppenberger, T. Wallimann, Novel thick filament protein of chicken pectoralis muscle: the 86 kd protein. II. Distribution and localization, J. Mol. Biol. 186 (1985) 393–401.
[21] P. Bennett, R. Craig, R. Starr, G. Offer, The ultrastructural location of C-protein, X-protein and H-protein in rabbit muscle, J. Muscle Res. Cell Motil. 7 (1986) 550–567.
[22] S. Schiaffino, C. Reggiani, Fiber types in mammalian skeletal muscles, Physiol. Rev. 91 (2011) 1447–1531.
[23] D. Pette, R.S. Staron, Transitions of muscle fiber phenotypic profiles, Histochem. Cell Biol. 115 (2001) 359–372.
[24] Y. Hosono, T. Yamaguchi, E. Mizutani, K. Yanagisawa, C. Arima, S. Tomida, Y. Shimada, M. Hiraoka, S. Kato, K. Yokoi, M. Suzuki, T. Takahashi, MYBPH, a transcriptional target of TTF-1, inhibits ROCK1, and reduces cell motility and metastasis, EMBO J. 31 (2011) 481–493.
[25] K. Riento, A.J. Ridley, Rocks: multifunctional kinases in cell behaviour, Nat. Rev. Mol. Cell Biol. 4 (2003) 446–456.
[26] M. Amano, M. Nakayama, K. Kaibuchi, Rho-kinase/ROCK: a key regulator of the cytoskeleton and cell polarity, Cytoskeleton (Hoboken) 67 (2010) 545–554.
[27] M.F. Olson, Applications for ROCK kinase inhibition, Curr. Opin. Cell Biol. 20 (2008) 242–248.
[28] R. Bowser, D. Lacomis, Applying proteomics to the diagnosis and treatment of ALS and related diseases, Muscle Nerve 40 (2009) 753–762.
[29] P.F. Pradat, M. Dib, Biomarkers in amyotrophic lateral sclerosis: facts and future horizons, Mol. Diagn. Ther. 13 (2009) 115–125.
[30] R.E. Welikson, D.A. Fischman, The C-terminal IgI domains of myosin-binding proteins C and H (MyBP-C and MyBP-H) are both necessary and sufficient for the intracellular crosslinking of sarcomeric myosin in transfected non-muscle cells, J. Cell Sci. 115 (2002) 3517–3526.
[31] J.D. Atkin, R.L. Scott, J.M. West, E. Lopes, A.K. Quah, S.S. Cheema, Properties of slow- and fast-twitch muscle fibres in a mouse model of amyotrophic lateral sclerosis, Neuromuscul. Disord. 15 (2005) 377–388.
[32] J.L. Gonzalez de Aguilar, C. Niederhauser-Wiederkehr, B. Halter, M. De Tapia, F. Di Scala, P. Demougin, L. Dupuis, M. Primig, V. Meininger, J.P. Loeffler, Gene profiling of skeletal muscle in an amyotrophic lateral sclerosis mouse model, Physiol. õGenomics 32 (2008) 207–218.
[33] D. Capitanio, M. Vasso, A. Ratti, G. Grignaschi, M. Volta, M. Moriggi, C. Daleno, C. Bendotti, V. Silani, C. Gelfi, Molecular signatures of amyotrophic lateral sclerosis disease progression in hind and forelimb muscles of an SOD1(G93A) mouse model, Antioxid. Redox Signal. 17 (2012) 1333–1350.
[34] H. Norman, J. Nordquist, P. Andersson, T. Ansved, X. Tang, B. Dworkin, L. Larsson, Impact of post-synaptic block of neuromuscular transmission, muscle unloading and mechanical ventilation on skeletal muscle protein and mRNA expression, Pflugers Arch. 453 (2006) 53–66.
[35] R.T. Jagoe, S.H. Lecker, M. Gomes, A.L. Goldberg, Patterns of gene expression in atrophying skeletal muscles: response to food deprivation, FASEB J. 16 (2002) 1697–1712.
[36] A. Ferrer-Martinez, E. Montell, M. Montori-Grau, C. Garcia-Martinez, A.M. Gomez-Foix, M.A. Roberts, R. Mansourian, K. Mace, Long-term cultured human myotubes decrease contractile gene expression and regulate apoptosis-related genes, Gene 384 (2006) 145–153.
[37] Y. Hosono, J. Usukura, T. Yamaguchi, K. Yanagisawa, M. Suzuki, T. Takahashi, MYBPH inhibits NM IIA assembly via direct interaction with NMHC IIA and reduces cell motility, Biochem. Biophys. Res. Commun. 428 (2012) 173–178.
[38] M.F. Olson, E. Sahai, The actin cytoskeleton in cancer cell motility, Clin. Exp. Metastasis 26 (2009) 273–287.
[39] M.S. Samuel, J.I. Lopez, E.J. McGhee, D.R. Croft, D. Strachan, P. Timpson, J. Munro, E. Schroder, J. Zhou, V.G. Brunton, N. Barker, H. Clevers, O.J. Sansom, K.I. Anderson, V.M. Weaver, M.F. Olson, Actomyosin-mediated cellular tension drives increased tissue stiffness and beta-catenin activation to induce epidermal hyperplasia and tumor growth, Cancer Cell 19 (2011) 776–791.